Metabolic Engineering Communications 8 (2019) e00085

Contents lists available at ScienceDirect

Metabolic Engineering Communications

journal homepage: www.elsevier.com/locate/mec

Controlled intracellular trafficking alleviates an expression bottleneck in *S. cerevisiae* ester biosynthesis

Jie Zhu[a], Cory Schwartz[b], Ian Wheeldon[b,c,*]

[a] *Biochemistry, University of California Riverside, Riverside, CA 92521, USA*
[b] *Chemical and Environmental Engineering, University of California Riverside, Riverside, CA 92521 USA*
[c] *Center for Industrial Biotechnology, Bourns College of Engineering, University of California Riverside, Riverside, CA 92521, USA*

ABSTRACT

In metabolic engineering, most available pathway engineering strategies aim to control enzyme expression by making changes at the transcriptional level with an underlying assumption that translation and functional expression follow suit. In this work, we engineer expression of a key reaction step in medium chain ester biosynthesis that does not follow this common assumption. The native *Saccharomyces cerevisiae* alcohol acyltransferses Eeb1 and Eht1 condense acyl-CoAs with ethanol to produce the corresponding ester, a reaction that is rate limiting in engineering ester biosynthesis pathways. By changing the N- and C-termini of Eeb1 to those of Eht1, Eeb1 localization is changed from the mitochondria to lipid droplets. The change has no significant effect on transcription, but increases protein expression by 23-fold thus enabling a 3-fold increase in enzyme activity. This system demonstrates one example of the impact of protein trafficking on functional pathway expression, and will guide future metabolic engineering of ester biosynthesis and, potentially, other pathways with critical membrane-bound enzymes.

1. Introduction

Over the past 15 years, we have witnessed a dramatic increase in our ability to control and regulate gene expression. The molecular techniques used to accomplish this are typically referred to as synthetic biology "tools". Collectively, the synthetic biology and metabolic engineering communities have developed large sets of standardized tools and genetic parts —promoters, terminators, ribosome binding sites, riboswitches — to control gene expression in the common microbial hosts *E. coli* and *S. cerevisiae* (Blazeck et al., 2012; Chen et al., 2013; Lee et al., 2015; Salis et al., 2009; Win and Smolke, 2007). Dynamic range can be greater than 1000-fold (Salis et al., 2009), inducibility and feedback regulation have been demonstrated (Xu et al., 2014; Zhang et al., 2012), and combinatorial refactoring of pathway expression is possible (Pfleger et al., 2006; Young et al., 2018). Genome-wide tools that create pooled libraries of mutants with targeted gene regulation have also been developed (e.g., MAGE, Tn-Seq, and TRMR; see (van Opijnen et al., 2009; Wang et al., 2009; Warner et al., 2010)). The recent discovery and widespread adoption of CRISPR-Cas9 and associated interference and activation systems (CRISPRi and CRISPRa) have enabled similar gene regulation abilities in a wide range of both model and non-conventional hosts (Löbs et al., 2017b; Schwartz et al., 2017b; Sidik et al., 2016).

These gene regulation tools are most often demonstrated (and standardized) with the model protein and fluorescent reporter GFP and its variants. Fluorescent proteins provide a useful functional screen to characterize newly developed tools: GFP is highly soluble, cytosolically expressed, and florescence readouts can readily provide quantifiable signals from bulk cultures and at the single cell level. The experimentally supported conclusion from the GFP model system is that transcription directly correlates with expression and function. That is, changes in transcript level produce equivalent changes in protein abundance and function. But given the complexities of protein expression, it is possible that a strong correlation between transcript level, protein abundance, and protein function will not be widely observed across the proteome (Liu et al., 2016; Payne, 2015; Vogel and Marcotte, 2012). Engineering more complex metabolic pathways and controlling polygenetic phenotypes will require fine control of protein function, and so a clearer understanding of the relationships between transcription, translation, and function in biotechnologically important systems is needed. To do so, we will need to consider intracellular localization, protein trafficking, protein degradation, and post translational modifications. Protein solubility can also affect overexpression

* Corresponding author.
E-mail address: iwheeldon@engr.ucr.edu (I. Wheeldon).

http://dx.doi.org/10.1016/j.mec.2018.e00085
Received 10 August 2018; Received in revised form 20 December 2018; Accepted 24 December 2018

profiles by limiting the amount of functional protein regardless of transcript level (Zhu et al., 2015).

Biosynthetic short and medium chain esters are valuable as natural food additives, industrial solvents, and alternatives to diesel fuel (Löbs et al., 2017b; Park et al., 2009). A number of different research groups have recently engineered synthetic pathways to convert fermentable sugars into a variety of different esters (Layton and Trinh, 2014; Löbs et al., 2016; Rodriguez et al., 2014; Steen et al., 2010); however, expression level tuning of the terminal reaction step catalyzed by alcohol-O-acetyl/acyltransferase (AATase) in both yeast and *E. coli* has proved to be challenging. In our own work, we have observed that heterologous expression of AATases in *E. coli* produces a positive correlation with respect to protein abundance, but a negative correlation for specific activity (Zhu et al., 2015). At increasing expression levels, enzyme aggregates formed due to poor solubility, which caused the reduction in specific activity. In *S. cerevisiae*, fatty acid ethyl ester (FAEE) production was not significant improved by overexpressing the AATases Eht1 and Eeb1 or by co-feeding fatty acid substrate (Saerens et al., 2006). The lack of improvement in the co-feeding experiments suggests that low FAEE production was due to poor enzyme activity and/or low expression and not due to limited substrate availability from upstream pathways.

In the work presented here, we demonstrate that native trafficking of the *S. cerevisiae* AATase Eeb1 to the mitochondria limits overexpression and ester biosynthesis activity. Eeb1 catalyzes the condensation of medium chain acyl-CoAs with an alcohol to produce the corresponding ester (Lin et al., 2016; Saerens et al., 2006). Its homolog, Eht1, exhibits different substrate selectivity and localizes to the endoplasmic reticulum (ER) before migrating to the surface of intracellular lipid droplets (LDs). Analysis of AATases in *S. cerevisiae* and other yeasts suggest that Eht1's trafficking is common among this enzyme family (Lin and Wheeldon, 2014). Given the similarities in Eeb1 and Eht1 function and the disparity in localization, we reasoned that this enzyme pair could be used to explore one example of how changes in localization and trafficking alter expression and enzyme activity (Fig. 1). By altering Eeb1's intracellular localization, we were able to alleviate the expression bottleneck and engineer a system that increased protein overexpression by 23-fold and produced a positive correlation between transcription, enzyme abundance, and enzyme activity.

2. Results and discussion

All strains and plasmids used to create a synthetic expression system for mitochondrial and LD localization of the alcohol acyltransferase Eeb1 are listed in Table 1.

Key to this study was the identification of N- and C-terminal domains that are necessary for Eeb1's mitochondrial localization and Eht1's localization to the ER and LDs (Fig. 2). Truncation experiments

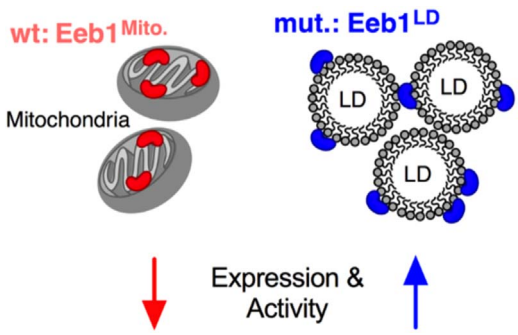

Fig. 1. Controlled intracellular localization alters the expression profile of the medium chain alcohol acyltransferase Eeb1 in *S. cerevisiae*. Wild type Eeb1 ($Eeb1^{Mito}$) localizes to the mitochondria, while the engineered mutant ($Eeb1^{LD}$) localizes to the surface of intracellular lipid droplets (LDs).

Table 1
Strains and plasmids used in this study.

Strains	Genotype	Source
E. coli		
DH5α	*F– Φ80lacZΔM15 Δ(lacZYA-argF) U169 recA1 endA1 hsdR17 (rK–, mK+) phoA supE44 λ– thi-1 gyrA96 relA1*	Life technologies
S. cerevisiae		
BY4742	*MATα his3Δ1 leu2Δ0 lys2Δ0 ura3Δ0*	GE healthcare
YS218	*MATα his3Δ1 leu2Δ0 lys2Δ0 ura3Δ0 ERG6::DsRed*	Lin 2014
YS578	*MATα his3Δ1 leu2Δ0 lys2Δ0 ura3Δ0 OM45::DsRed*	this study

plasmid	description	source
pEEB1	pRS426-P_{PGK1}-EEB1-GFP-T_{PGK1}	this study
pEEB2	pRS426-P_{PGK1}-EHT1 (1–13AA)-EEB1 (14–456AA)-GFP-T_{PGK1}	this study
pEEB3	pRS426-P_{PGK1}-EEB1 (1–433AA)-EHT1 (429–451AA)-GFP-T_{PGK1}	this study
pEEB4	pRS426-P_{PGK1}-EHT1 (1–13AA)-EEB1 (14–433AA)-EHT1 (429–451AA)-GFP-T_{PGK1}	this study
pEEB5	pRS316-P_{REV1}-EEB1-GFP-T_{PGK1}	this study
pEEB6	pRS316-P_{TPI1}-EEB1-GFP-T_{PGK1}	this study
pEEB7	pRS316-P_{PGK1}-EEB1-GFP-T_{PGK1}	this study
pEEB8	pRS316-P_{TEF1}-EEB1-GFP-T_{PGK1}	this study
pEEB9	pRS316-P_{REV1}-EHT1 (1–13AA)-EEB1 (14–433AA)-EHT1 (429–451AA)-GFP-T_{PGK1}	this study
pEEB10	pRS316-P_{TPI1}-EHT1 (1–13AA)-EEB1 (14–433AA)-EHT1 (429–451AA)-GFP-T_{PGK1}	this study
pEEB11	pRS316-P_{PGK1}-EHT1 (1–13AA)-EEB1 (14–433AA)-EHT1 (429–451AA)-GFP-T_{PGK1}	this study
pEEB12	pRS316-P_{TEF1}-EHT1 (1–13AA)-EEB1 (14–433AA)-EHT1 (429–451AA)-GFP-T_{PGK1}	this study

revealed that the loss of amino acids 1–13 and 434–456 in Eeb1 and the loss of 1–13 and 429–451 in Eht1 resulted in cytosolic expression. To investigate the potential of using these different terminal domains to drive changes in localization, we first created LD and mitochondrial marker strains by genetically fusing the red fluorescent protein DsRed to the chromosomal copies of *ERG6* and *OM45*, LD and mitochondrial markers, respectively. The fluorescence microscopy images shown in Fig. 2B revealed that the Eht1 domains impart LD localization on Eeb1. Wild type Eeb1 ($Eeb1^{Mito}$) with a C-terminally fused GFP colocalized with OM45-DsRed, indicating mitochondrial targeting. GFP tagged Eht1 colocalized with the LD marker Erg6-DsRed. Mutant $Eeb1^{LD}$, in which the native terminal domains were swapped with those of Eht1, exhibited similar targeting as Eht1 colocalizing with Erg6-DsRed on the outer surface of intracellular LDs. Translating the Eeb1 termini to Eht1 was less successful; fusion of the N-terminus produced a growth defect and the enzyme remained partially localized to the ER and LDs, while Eht1 with the Eeb1 C-terminal domain resulted in cytosolic localization (Supporting Fig. 1). Given these results, we did not pursue Eht1 targeting to the mitochondria.

Time course studies of the intracellular localization of $Eeb1^{Mito}$ and $Eeb1^{LD}$ at time points of 4, 10, 18, and 24 h were performed to study their cellular trafficking (Fig. 2C). In lag and early log phases (4 and 10 h in baffled shake flasks, respectively), $Eeb1^{LD}$ showed clear ER structure. At the same time points $Eeb1^{Mito}$ was localized to the cytosol and the ER. As cells moved to late log and early stationary phases (18 and 24 h, respectively), $Eeb1^{LD}$ trafficked from the ER to LDs, while $Eeb1^{Mito}$ localized to mitochondria. To determine if $Eeb1^{Mito}$ and $Eeb1^{LD}$ were membrane associated as suggested by fluorescence microscopy, we examined their fractionation pattern in differential centrifugation (Fig. 2D). Western blot analysis showed that both Eeb1 variants were enriched in a 13,000*g* pellet, which collects the membrane fraction of lysed cells. A small amount of cytosolic partitioning was also observed for both $Eeb1^{Mito}$ and $Eeb1^{LD}$.

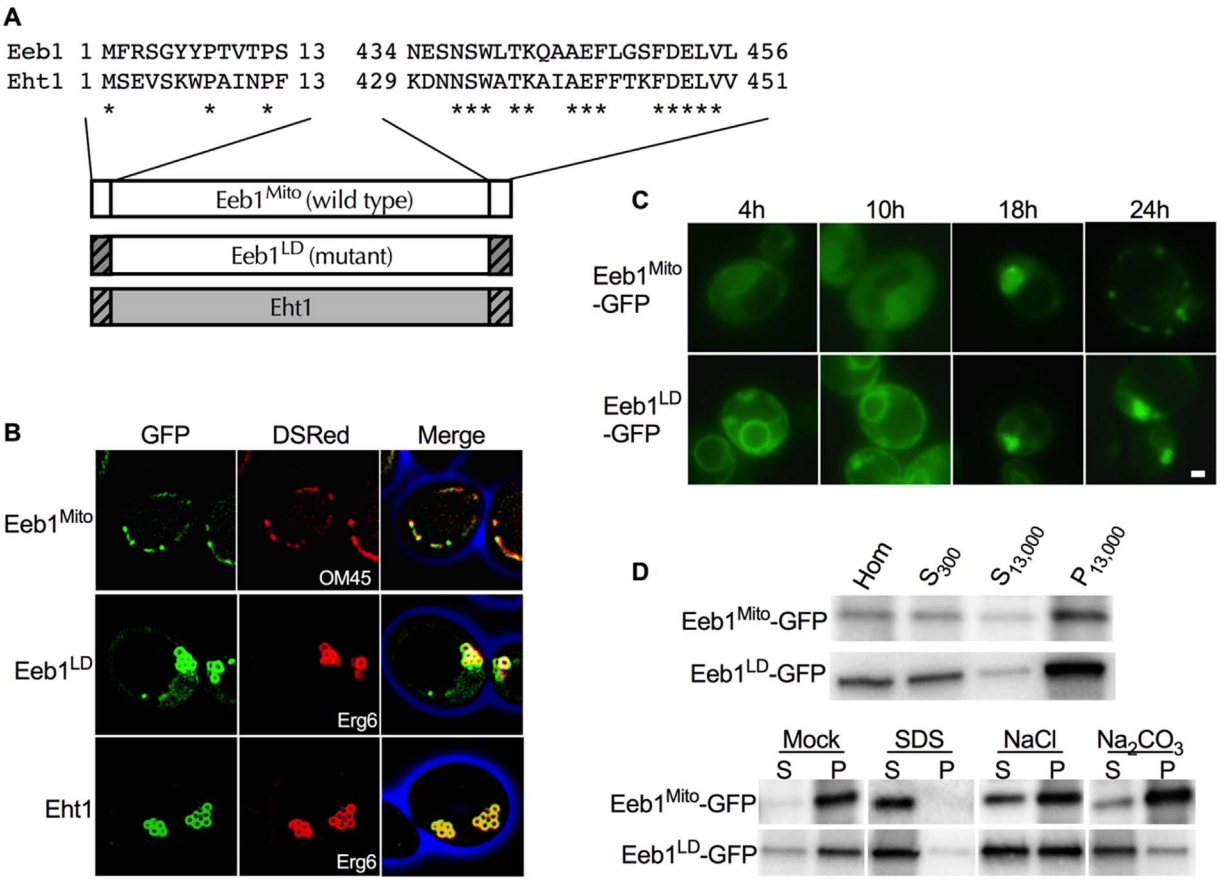

Fig. 2. Protein engineering of Eeb1 imparts LD intracellular localization. (A) N- and C-terminal amino acid sequences of Eeb1 and Eht1 along with the Eeb1^{LD} mutant that contains Eht1 terminal sequences. (B) Fluorescence microscopy of *S. cerevisiae* expressing Eeb1 variants (Eeb1^{Mito} and Eeb1^{LD}) and Eht1 with fused GFP (green). Mitochondria are identified with an OM45-DsRed protein marker (red), while LDs are identified with Erg6-DsRed (red). Images were acquired using a 100x objective and merged images of green fluorescence, red fluorescence, and phase contrast (blue) are shown. Yellow indicates colocalization of red and green fluorescence. (C) Green fluorescence images of *S. cerevisiae* expressing Eeb1^{Mito}-GFP and Eeb1^{LD}-GFP at 4, 10, 18 and 24 h. Scale bar is 1 μm. (D) Analysis of Eeb1 membrane association. Early log phase cells overexpressing Eeb1-GFP variants were isolated and disrupted by Dounce homogenization (Hom), the soluble fraction was removed (S_{300}), membrane fractions were pelleted by centrifugation at 13,000*g* ($P_{13,000}$) and compared to the soluble fraction ($S_{13,000}$). 50 μg of protein from the membrane pellet was treated at 4 °C with 1 M NaCl, 0.1 M Na_2CO_3, 1% SDS, or buffer alone (Mock) and then centrifuged at 13,000*g* for 30 min to yield soluble (S) and pellet (P) fractions (For interpretation of the references to color in this figure legend, the reader is referred to the web version of this article).

To further characterize the native and engineering membrane association of Eeb1, the isolated 13,000 *g* membrane fractions were treated with chemicals that disrupt membrane association (Fig. 2D). In samples incubated with buffer alone (Mock), Eeb1^{Mito} and Eeb1^{LD} were found almost exclusively in the insoluble pellet (P) fraction. In the presence of detergent (1% SDS), Eeb1^{Mito} and Eeb1^{LD} were completely solubilized. In contrast, the presence of 1 M sodium chloride or 0.1 M sodium carbonate, conditions known to solubilize peripheral membrane proteins (see (Koffel et al., 2005)), partially solubilized Eeb1^{Mito} and Eeb1^{LD} suggesting that both are peripheral membrane proteins. Of note is that ~10% of Eeb1^{Mito} and ~75% of Eeb1^{LD} were released from the membrane pellets treated with sodium carbonate. This suggests that the membrane interactions of the wild type and mutant have different binding strengths to their associated membranes.

The engineered Eeb1^{Mito}/Eeb1^{LD} enzyme pair allowed us to test the effects of controlled intracellular trafficking and localization on protein expression and activity towards ethyl ocatonate biosynthesis via an acyltransferase reaction (Fig. 3A). We first created a series of variable expression promoters using multicopy 2μ-based plasmids (Table 1). The promoter series of REV1, TPI1, PGK1, and TEF1 combined with a CYC1 terminator produced a transcriptional range of over 20-fold (Fig. 3B and C), and each promoter was used to express Eeb1^{Mito} and Eeb1^{LD} with transcript level, protein abundance, and enzymatic activity measured for each experimental condition.

Western blot analysis revealed that wild type Eeb1 (Eeb1^{Mito}) protein level was insensitive to transcriptional level in the tested range, while LD localized Eeb1 (Eeb1^{LD}) increased with increasing transcription (Fig. 3C). At the highest transcriptional level (achieved with the TEF1/CYC1 expression cassette) Eeb1^{LD} abundance was 23-fold higher than Eeb1^{Mito}. Enzymatic activity measured in cell lysate assays revealed a similar trend; increased transcription did not increase the observed activity of Eeb1^{Mito}, but Eeb1^{LD} activity increased with transcript abundance (Fig. 3D). The result was that the specific activity of Eeb1^{Mito} was fixed at a low level (2.0 ± 0.01 nmol min^{-1}mg^{-1}), but Eeb1^{LD} activity was controllable within a range of 2.5 ± 0.4–6.1 ± 0.6 nmol min^{-1} mg^{-1} (Fig. 3E). It is important to note that enzyme activity was not enhanced to the same degree as protein expression. The difference between increased enzyme abundance (as measured by Western blot analysis, see Supporting Fig. 2) and measured ester biosynthesis activity (evaluated in lysate assays) may be due to thioesterase activity and/or ethanol inhibition, both of which are common in yeast AATases (Kruis et al., 2017; Nancolas et al., 2017).

One possible explanation for the difference in expression and activity profiles of Eeb1^{Mito} and Eeb1^{LD} is increased protein degradation resulting from altered intracellular trafficking. As such, we conducted a time-course protein degradation study comparing the two Eeb1 variants. The fluorescence-based assay monitored GFP tagged Eeb1 levels after chemical inhibition of protein translation by cycloheximide and revealed that 25% of expressed Eeb1^{Mito} and Eeb1^{LD} degraded over a 4-h period (Fig. 4). The degradation profiles were also similar. These results suggest that differences in protein degradation was not a contributing factor in enhancing protein

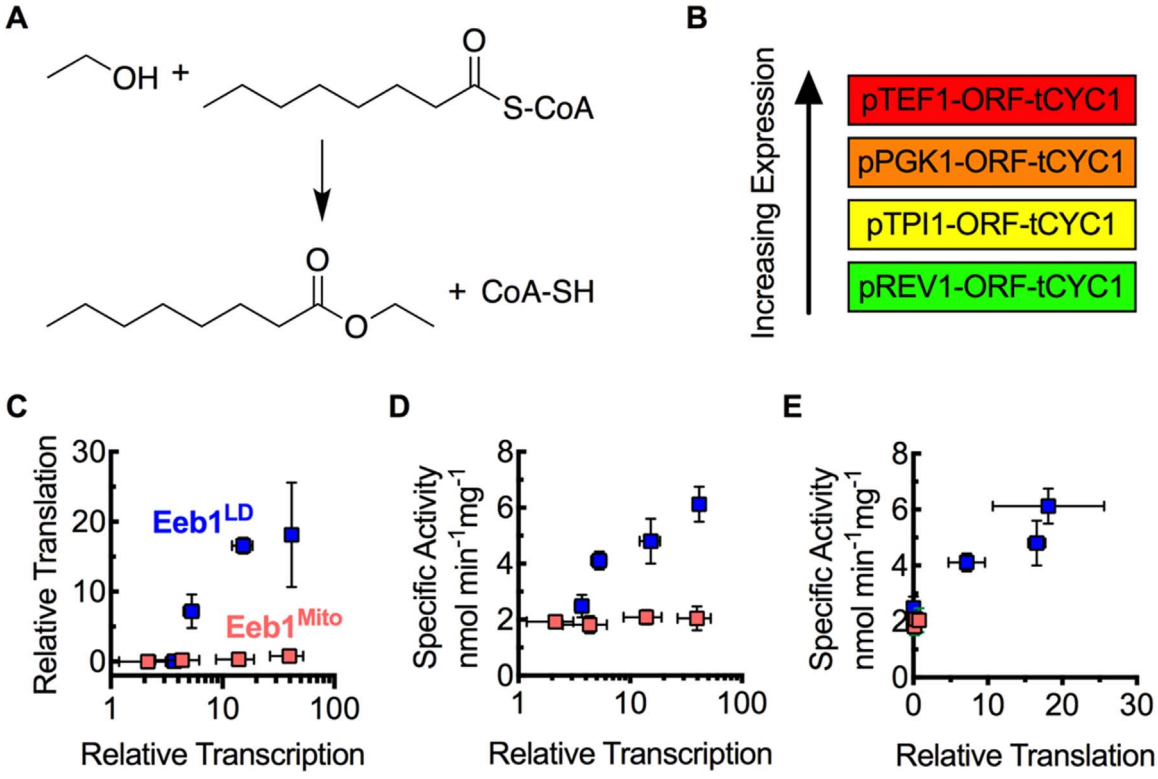

Fig. 3. Translational and functional tuning of Eeb1 through controlled intracellular localization. (A) Ethyl octanoate synthesis by Eeb1-mediated condensation of ethanol and octanoyl-CoA. (B) Variable expression level promoter series used to tune expression of Eeb1 variants. (C, D, E) Protein abundance and activity of $Eeb1^{Mito}$ and $Eeb1^{LD}$ as a function of transcriptional and translational levels. Specific activity is shown in units of nmol min^{-1} mg^{-1} of cell lysate protein. Transcriptional level is presented relative to constitutive expression of *TAF10* and protein abundance is shown relative to a GAPDH control in each analyzed sample. Each data point represents the mean and standard deviation of biological triplicates.

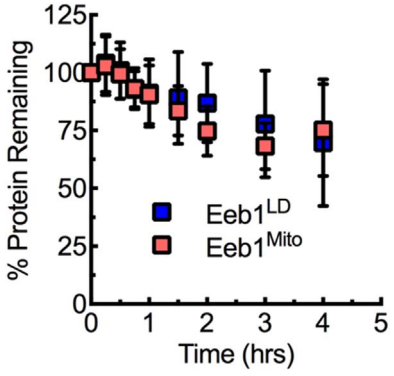

Fig. 4. $Eeb1^{Mito}$ and $Eeb1^{LD}$ degradation after chemical inhibition of protein translation. Two-way ANOVA indicates that there is an effect of time but there is no statistical difference between Eeb1 variants $Eeb1^{Mito}$ and $Eeb1^{LD}$ (Two-way ANOVA: time, $p < 0.0001$, $n = 3$; Eeb1 variant, $p = 0.82$, $n = 3$). Protein remaining was measure by measured GFP fluorescence normalized to the fluorescence signal at $t = 0$ h. Cycloheximide (250 μg mL^{-1}) was used to inhibit translation.

expression and function of $Eeb1^{LD}$.

Post-translational modifications of Eeb1 (or other yeast alcohol acetyl/acyltransferases) have not been identified and based on the minimal amino acid sequence changes between $Eeb1^{Mito}$ and $Eeb1^{LD}$, it is unlikely that post-translational modifications significantly influenced expression and function. Western blot analysis of the soluble and insoluble fractions of $Eeb1^{LD}$-GFP and $Eeb1^{Mito}$-GFP expression strains indicated similar ratios of soluble and insoluble protein, thus suggesting that terminal domain swapping did not significantly alter protein solubility and that changes in solubility can be ruled out as the cause of increased expression. The data presented in this study provides strong evidence that trafficking and localization are the primary bottleneck for wild type Eeb1 expression. By fusing the N- and C-terminal domains of Eht1 to Eeb1, the Eeb1 mutant is first targeted to the ER (Fig. 2C) and subsequently localized to the outer surface of intracellular LDs (Fig. 2B). Wild type localization is to the mitochondria. This altered trafficking and localization resulted in a synthetic enzyme expression system that maintained a positive correlation between transcript level, protein abundance, and enzyme activity, a correlation that was not observed when the wild type enzyme followed its native trafficking pattern to the mitochondria (Fig. 3C, D, and E).

Proteomic analyses of eukaryotes show that global assumptions about the linear correlations between transcription and protein expression can be problematic. In general, there is a positive correlation between transcript and protein abundance, but analyses reveal a weak correlation (e.g., Pearson coefficients, a metric for evaluating linear correlations, range from ~0.4 to ~0.7 for the *S. cerevisiae* proteome, see refs (Vogel and Marcotte, 2012) and (Liu et al., 2016) and the references therein). A common metabolic engineering solution to such expression problems is to identify alternative enzymes with the desired activity but with more favorable expression profiles. This strategy, however, is not always possible, especially with membrane-bound proteins. Our previous work with various alcohol acetyl/acyltransferases (ATTases) is a good example of this because membrane association is critical for high activity and poor solubility limits high level expression (Zhu et al., 2015). The broad class of membrane-bound P450 monooxygenases are another good example as many of these enzymes are critical to the biosynthesis of secondary metabolites with high value as pharma- and nutraceuticals (Li and Smolke, 2016; Mora-Pale et al., 2014; Galanie et al., 2015). Limited expression profiles are also likely to be found in other membrane-bound and organelle-targeted enzymes that will be used in future metabolic engineering efforts to translate complex biosynthetic pathways to microbial hosts that are suitable for industrial bioprocessing (Löbs et al., 2017a; Mora-Pale et al., 2014; Schwartz et al., 2017a; Wheeldon

et al., 2017). The engineered intracellular localization strategy presented here addresses a specific problem with Eeb1 mitochondrial targeting, but also outlines a pathway engineering approach that may find utility in alleviating expression bottlenecks in other pathways with key reactions step targeted to mitochondria or other organelles.

In this work, we developed a strategy that alleviates an expression bottleneck cause by intracellular localization by altering enzyme trafficking and terminal localization of the enzyme of interest. This was made possible through protein engineering to the enzyme, Eeb1 from *S. cerevisiae*, to alter the N- and C-terminal localization tags. The new terminal domains were identified from a similar AATase found in *S. cerevisiae*, Eht1, which natively localizes to intracellular LDs. Domain swapping of Eht1 and Eeb1 resulted in an Eeb1 mutant with intracellular localization that differed from the wild type. $Eeb1^{Mito}$, the wild type enzyme, localized to the mitochondria, while $Eeb1^{LD}$, the mutant enzyme with N- and C-terminal domains from Eht1, localized to the ER and finally to LDs. The result of the change in localization was the recovery of a positive correlation between transcription, protein abundance, and enzyme activity. The altered localization also introduces the possibility of exploiting enzyme colocalization strategies to increase pathway flux as was previously accomplished for the overproduction of ethyl acetate in yeast (Lin et al., 2017). Eeb1 localization to the outer surface of lipid droplets also presents the potential advantage of colocalization with fatty acid substrates released from the lipase-mediated mobilization of lipids sequestered in triacylglycerides (TAGs). The engineered system of $Eeb1^{LD}$ could now be used to alter the flavor and fragrance profile of *S. cerevisiae* fermented beverages or could be used to optimize enzyme expression levels in a biosynthesis pathway for fatty acid ethyl esters and medium chain volatile esters (Eriksen et al., 2015; Rodriguez et al., 2014; Runguphan and Keasling, 2014; Thompson and Trinh, 2014).

3. Conclusion

This work develops a protein engineering solution to an important technical challenge in metabolic engineering, tuning of expression and activity profiles of a membrane-associated enzyme critical to a desired biosynthetic pathway. Typically, expression tuning is accomplished by varying promoter strength in an engineered overexpression cassette, but in the case of Eeb1 (an AATase that catalyzes the condensation of an alcohol with medium chain acyl-CoA) increased transcript level did not result in increased protein expression or function. By changing the N- and C-terminal localization domains, we were able to eliminate native Eeb1 localization to the mitochondria and engineer targeting to intracellular LDs. Localization to LDs maintains membrane association that is necessary for high enzyme activity in this class of enzymes (Zhu et al., 2015), and alleviated the expression bottleneck. The result was that Eeb1 expression was increased by up to 23-fold over the wild type and that enzyme activity could now be increased by up to 3-fold. The work presented here is a solution specific to Eeb1, but represents a possible route to alleviating expression bottlenecks in other membrane-bound enzymes critical to metabolic engineering.

4. Materials and methods

4.1. Strains and culture conditions

All *S. cerevisiae* and *E. coil* strains used in this work are summarized in Table 1. All modified yeast strains were derived from laboratory strains BY4742 (Brachmann et al., 1998). *E. coli* DH5α grown in Luria Broth (LB; Sigma-Aldrich) containing 50 μg mL^{-1} ampicillin (Fisher Scientific) was used for molecular cloning. *S. cerevisiae* strains without plasmids were grown in YPD media containing 10 g L^{-1} yeast extract, 20 g L^{-1} peptone, and 20 g L^{-1} glucose (Sigma-Aldrich) in baffled shake flask with 25 mL of culture volume. *S. cerevisiae* strains harboring plasmids were grown in synthetic complete media without uracil (SC-U) containing 6.7 g L^{-1} yeast nitrogen (Becton-Dickinson), 2 g L^{-1} synthetic dropout mix without uracil (Sigma-Aldrich), and 20 g L^{-1} glucose (Sigma-Aldrich). When necessary, solid media were prepared as above with 20 g L^{-1} agar. All yeast cultures were grown at 30 °C, while *E. coli* cultures for molecular cloning were grown at 37 °C.

4.2. Plasmid and yeast strain construction

All yeast genes, promoters, and terminators were amplified from *S. cerevisiae* genomic DNA. The peptide tags used for western blot were incorporated into proteins by including the DNA sequence in the appropriate PCR amplification primers.

The plasmids used in this study are listed in Table 1 and were transformed into yeast using a standard PEG/LiAC protocol (Gietz and Woods, 2002). The following outlines the construction of the overexpression plasmids for the REV1, TPI1, PGK1, and TEF1 promoter series used to express $Eeb1^{Mito}$ and $Eeb1^{LD}$ with C-terminally fused GFP. The promoters and terminator were amplified from genomic DNA of BY4742 and cloned into 2μ-based plasmid pRS426. The promoter was inserted using SacI and SacII sites, while CYC1t was inserted using SpeI and KpnI sites. GFP was inserted at the 3′ end of the Eeb1coding region using NotI and SpeI sites. Wildtype $Eeb1^{Mito}$ and the domain swap variant $Eeb1^{LD}$ were inserted using SacII and NotI sites. Terminal domain swapping of Eht1 and Eeb1 was accomplished by PCR and changing the sequences on the primers. Forward primer used was 5′-ATATCCCCGCGG*ATGTCAGAAGTTTCCAAATGGCCAGCAATCAACCC-ATTC*CATTGGGGCTATAACGGCAC-3′; the reverse primer used was 5′-AAAAGTAAAGCGGCCGC*CTACGACTAATTCATCAAACTTAGTGAAAA-ATTCTGCAATTGCCTTGGTAGCCCACGAGTTGTTGTCTTT*GTCGAGA-TAAGCCAAATGTCCAC-3′ (underlined nucleotides showed the restriction enzyme sites SacII and NotI; italic nucleotides showed the swap sequences from Eht1).

DsRed, amplified from pERGmDsRed (gift from J. Goodman, University of Texas Southwestern Medical School), was first inserted into pRS426 containing PGK1p-PGK1t at NotI and SpeI sites. LEU2, amplified from pRS315, was subsequently inserted between KpnI and EcoRV sites. This cassette was used to fuse DsRed to the 3′ end of the LD marker Erg6 and the mitochondria marker OM45 by PCR-based homologous recombination as previously described (Lin and Wheeldon, 2014).

4.3. Fluorescence microscopy analysis

Cells were imaged using an Olympus BX51 microscope (UPlanFL 100 × 1.30 oil-immersion objective lens, mercury lamp) and fluorescence micrographs were captured by a Q-Imaging Retiga Exi CCD camera. Images were processed using CellSens Dimension 1.7 software (Olympus). In all cases, at least three cell populations were analyzed and images representative of the cell populations are shown.

4.4. Subcellular fractionation and membrane topology assay

Fractionation on an Accudenz density gradient was performed as described by Cowles et al. (1997). Briefly, 100 OD units of early log phase cells were harvested and transformed into spheroplasts by zymolyase 20 T (Seikagaku Corporation). Spheroplasts were resuspended in lysis buffer (0.25 M sorbitol, 10 mM MES-Tris pH 6.9, and 0.2 mM EDTA) supplemented with a protease inhibitor cocktail (Roche), and lysed with a Dounce homogenizer by 40 strokes. Homogenates were precleared by centrifugation at 300*g* for 10 min, then separated into pellet and supernatant fractions by centrifugation at 13,000*g* for 20 min. All centrifugation steps were performed at 4 °C.

To determine the membrane association, detergent and salt extractions of microsomal membranes were performed by incubating 50 μg of the microsomal fraction with 1% SDS, 1 M NaCl, or 0.1 M Na_2CO_3 in

lysis buffer for 30 min on ice (Koffel et al., 2005). Samples were then centrifuged at 13,000*g* for 10 min, and proteins from the pellet and supernatant fractions were precipitated by 10% TCA and analyzed by Western blotting. Protein concentrations were determined by a commercially available assay (Pierce 660 nm Protein Assay; Thermo Fisher) and quantified with Nanodrop 2000c.

4.5. Western blot analysis

Western blots were performed using standard procedure. Briefly, proteins were loaded on Any kD™ Mini-PROTEAN® TGX™ Gel (Bio-Rad) and run at 200 V for 30 min. Samples were electrophoretically transferred to a PVDF membrane at 25 V overnight. Membranes were blocked with 5% non-fat milk in Tris buffer saline with TWEEN-20 (TBST) buffer for 1 h at room temperature, washed, and incubated with primary antibody in TBST with 1% non-fat milk for 1 h. Secondary antibody in TBST with 1% non-fat milk was applied, and incubated at room temperature for 0.5 h. After washing with TBST, Immobilon Western HRP Substrate (Millipore) was used for signal detection and UN-SCAN-IT gel 6.1 software was used to quantify band intensity. The following antibodies were used: rabbit anti-GFP (NB600-303; Novusbio), mouse anti-Myc (SC-40; Santa Cruz Biotech), goat anti-rabbit IgG-HRP (65–6120; Invitrogen), goat anti-mouse IgG-HRP (31430; Thermo Fisher Scientific).

4.6. Protein degradation assay

Protein degradation assays were performed using a standard protocol for cycloheximide chase assays (Buchanan et al., 2016). Briefly, yeast cells were grown to exponential phase at which point 250 $\mu g\,mL^{-1}$ of cycloheximide was added. GFP fluorescence from $Eeb1^{LD}$-GFP and $Eeb1^{Mito}$-GFP was measured using a microtiter fluorescence plate reader at desired time intervals to monitor change in fluorescence and GFP degradation. Fluorescence values were normalized to cell density, and each data point was collected from biological triplicates.

Acknowledgements

The authors thank the Army Research Office MURI (W911NF1410263) and the National Science Foundation (NSF-1803630) for financial support.

Appendix A. Supplementary material

Supplementary data associated with this article can be found in the online version at doi:10.1016/j.mec.2018.e00085.

References

Blazeck, J., Garg, R., Reed, B., Alper, H.S., 2012. Controlling promoter strength and regulation in Saccharomyces cerevisiae using synthetic hybrid promoters. Biotechnol. Bioeng. 109, 2884–2895.
Brachmann, C.B., Davies, A., Cost, G.J., Caputo, E., Li, J., Hieter, P., Boeke, J.D., 1998. Designer deletion strains derived from Saccharomyces cerevisiae S288C: a useful set of strains and plasmids for PCR-mediated gene disruption and other applications. Yeast 14, 115–132.
Buchanan, B.W., Lloyd, M.E., Engle, S.M., Rubenstein, E.M., 2016. Cycloheximide chase analysis of protein degradation in saccharomyces cerevisiae. Jove-J. Vis. Exp..
Chen, Y.J., Liu, P., Nielsen, A.A.K., Brophy, J.A.N., Clancy, K., Peterson, T., Voigt, C.A., 2013. Characterization of 582 natural and synthetic terminators and quantification of their design constraints. Nat. Methods 10, 659, (-+).
Cowles, C.R., Odorizzi, G., Payne, G.S., Emr, S.D., 1997. The AP-3 adaptor complex is essential for cargo-selective transport to the yeast vacuole. Cell 91, 109–118.
Eriksen, D.T., HamediRad, M., Yuan, Y.B., Zhao, H.M., 2015. Orthogonal fatty acid biosynthetic pathway improves fatty acid ethyl ester production in saccharomyces cerevisiae. ACS Synth. Biol. 4, 808–814.
Galanie, S., Thodey, K., Trenchard, I.J., Interrante, M.F., Smolke, C.D., 2015. Complete biosynthesis of opioids in yeast. Science 349, 1095–1100.
Gietz, R.D., Woods, R.A., 2002. Transformation of yeast by lithium acetate/single-stranded carrier DNA/polyethylene glycol method. Transformation of yeast by lithium acetate/single-stranded carrier DNA/polyethylene glycol method. Methods Enzymol. Pt B 350, 87–96.
Koffel, R., Tiwari, R., Falquet, L., Schneiter, R., 2005. The Saccharomyces cerevisiae YLL012/YEH1, YLR020/YEH2, and TGL1 genes encode a novel family of membrane-anchored lipases that are required for steryl ester hydrolysis. Mol. Cell Biol. 25, 1655–1668.
Kruis, A.J., Levisson, M., Mars, A.E., van der Ploeg, M., Daza, F.G., Ellena, V., Kengen, S.W.M., van der Oost, J., Weusthuis, R.A., 2017. Ethyl acetate production by the elusive alcohol acetyltransferase from yeast. Metab. Eng. 41, 92–101.
Layton, D.S., Trinh, C.T., 2014. Engineering modular ester fermentative pathways in Escherichia coli. Metab. Eng. 26, 77–88.
Lee, M.E., DeLoache, W.C., Cervantes, B., Dueber, J.E., 2015. A highly characterized yeast toolkit for modular, multipart assembly. ACS Synth. Biol. 4, 975–986.
Li, Y.R., Smolke, C.D., 2016. Engineering biosynthesis of the anticancer alkaloid noscapine in yeast. Nat. Commun. 7.
Lin, J.L., Wheeldon, I., 2014. Dual N- and C-terminal helices are required for endoplasmic reticulum and lipid droplet association of alcohol acetyltransferases in Saccharomyces cerevisiae. PLoS One 9, e104141.
Lin, J.L., Zhu, J., Wheeldon, I., 2016. Rapid ester biosynthesis screening reveals a high activity alcohol-O-acyltransferase (AATase) from tomato fruit. Biotechnol. J. 11, 700–707.
Lin, J.L., Zhu, J., Wheeldon, I., 2017. Synthetic protein scaffolds for biosynthetic pathway colocalization on lipid droplet membranes. ACS Synth. Biol. 6, 1534–1544.
Liu, Y.S., Beyer, A., Aebersold, R., 2016. On the dependency of cellular protein levels on mRNA abundance. Cell 165, 535–550.
Löbs, A.K., Engel, R., Schwartz, C., Flores, A., Wheeldon, I., 2017b. CRISPR-Cas9-enabled genetic disruptions for understanding ethanol and ethyl acetate biosynthesis in Kluyveromyces marxianus. Biotechnol. Biofuels 10, 164.
Löbs, A.-K., Lin, J.-L., Cook, M., Wheeldon, I., 2016. High throughput, colorimetric screening of microbial ester biosynthesis reveals high ethyl acetate production from Kluyveromyces marxianus on C5, C6, and C12 carbon sources. Biotechnol. J. 11, 1274–1281.
Löbs, A.-K., Schwartz, C., Wheeldon, I., 2017a. Genome and metabolic engineering in non-conventional yeasts: current advances and applications. Synth. Syst. Biotechnol. 2, 198–207.
Mora-Pale, M., Sanchez-Rodriguez, S.P., Linhardt, R.J., Dordick, J.S., Koffas, M.A.G., 2014. Biochemical strategies for enhancing the in vivo production of natural products with pharmaceutical potential. Curr. Opin. Biotechnol. 25, 86–94.
Nancolas, B., Bull, I.D., Stenner, R., Dufour, V., Curnow, P., 2017. Saccharomyces cerevisiae Atf1p is an alcohol acetyltransferase and a thioesterase in vitro. Yeast 34, 239–251.
Park, Y.C., Shaffer, C.E.H., Bennett, G.N., 2009. Microbial formation of esters. Appl. Microbiol. Biot. 85, 13–25.
Payne, S.H., 2015. The utility of protein and mRNA correlation. Trends Biochem. Sci. 40, 1–3.
Pfleger, B.F., Pitera, D.J., D Smolke, C., Keasling, J.D., 2006. Combinatorial engineering of intergenic regions in operons tunes expression of multiple genes. Nat. Biotechnol. 24, 1027–1032.
Rodriguez, G.M., Tashiro, Y., Atsumi, S., 2014. Expanding ester biosynthesis in Escherichia coli. Nat. Chem. Biol. 10, 259–265.
Runguphan, W., Keasling, J.D., 2014. Metabolic engineering of Saccharomyces cerevisiae for production of fatty acid-derived biofuels and chemicals. Metab. Eng. 21, 103–113.
Saerens, S.M.G., Verstrepen, K.J., Van Laere, S.D.M., Voet, A.R.D., Van Dijck, P., Delvaux, F.R., Thevelein, J.M., 2006. The Saccharomyces cerevisiae EHT1 and EEB1 genes encode novel enzymes with medium-chain fatty acid ethyl ester synthesis and hydrolysis capacity. J. Biol. Chem. 281, 4446–4456.
Salis, H.M., Mirsky, E.A., Voigt, C.A., 2009. Automated design of synthetic ribosome binding sites to control protein expression. Nat. Biotechnol. 27, 946–U112.
Schwartz, C., Frogue, K., Misa, J., Wheeldon, I., 2017a. Host and pathway engineering for enhanced lycopene biosynthesis in Yarrowia lipolytica. Front. Microbiol. 8.
Schwartz, C., Frogue, K., Ramesh, A., Misa, J., Wheeldon, I., 2017b. CRISPRi repression of nonhomologous end-joining for enhanced genome engineering via homologous recombination in Yarrowia lipolytica. Biotechnol. Bioeng. 114, 2896–2906.
Sidik, S.M., Huet, D., Ganesan, S.M., Huynh, M.H., Wang, T., Nasamu, A.S., Thiru, P., Saeij, J.P.J., Carruthers, V.B., Niles, J.C., Lourido, S., 2016. A genome-wide CRISPR screen in toxoplasma identifies essential apicomplexan genes. Cell 166, 1423–1435.
Steen, E.J., Kang, Y.S., Bokinsky, G., Hu, Z.H., Schirmer, A., McClure, A., del Cardayre, S.B., Keasling, J.D., 2010. Microbial production of fatty-acid-derived fuels and chemicals from plant biomass. Nature 463, 559–U182.
Thompson, R.A., Trinh, C.T., 2014. Enhancing fatty acid ethyl ester production in Saccharomyces cerevisiae through metabolic engineering and medium optimization. Biotechnol. Bioeng. 111, 2200–2208.
van Opijnen, T., Bodi, K.L., Camilli, A., 2009. Tn-seq: high-throughput parallel sequencing for fitness and genetic interaction studies in microorganisms. Nat. Methods 6, 767–772.
Vogel, C., Marcotte, E.M., 2012. Insights into the regulation of protein abundance from proteomic and transcriptomic analyses. Nat. Rev. Genet. 13, 227–232.
Wang, H.H., Isaacs, F.J., Carr, P.A., Sun, Z.Z., Xu, G., Forest, C.R., Church, G.M., 2009. Programming cells by multiplex genome engineering and accelerated evolution. Nature 460, 894–898.
Warner, J.R., Reeder, P.J., Karimpour-Fard, A., Woodruff, L.B.A., Gill, R.T., 2010. Rapid profiling of a microbial genome using mixtures of barcoded oligonucleotides. Nat. Biotechnol. 28, 856–U138.
Wheeldon, I., Christopher, P., Blanch, H., 2017. Integration of heterogeneous and

biochemical catalysis for production of fuels and chemicals from biomass. Curr. Opin. Biotechnol. 45, 127–135.
Win, M.N., Smolke, C.D., 2007. A modular and extensible RNA-based gene-regulatory platform for engineering cellular function. Proc. Natl. Acad. Sci. USA 104, 14283–14288.
Xu, P., Li, L.Y., Zhang, F.M., Stephanopoulos, G., Koffas, M., 2014. Improving fatty acids production by engineering dynamic pathway regulation and metabolic control. Proc. Natl. Acad. Sci. USA 111, 11299–11304.
Young, E.M., Zhao, Z., Gielesen, B.E.M., Wu, L., Benjamin Gordon, D., Roubos, J.A., Voigt, C.A., 2018. Iterative algorithm-guided design of massive strain libraries, applied to itaconic acid production in yeast. Metab. Eng. 48, 33–43.
Zhang, F.Z., Carothers, J.M., Keasling, J.D., 2012. Design of a dynamic sensor-regulator system for production of chemicals and fuels derived from fatty acids. Nat. Biotechnol. 30, 354–359.
Zhu, J., Lin, J.-L., Palomec, L., Wheeldon, I., 2015. Microbial host selection affects intracellular localization and activity of alcohol-O-acetyltransferase. Microb. Cell Factor 14, 35.